Coupling numerical and experimental methods to characterise the mechanical behaviour of the *Mona Lisa*: a method to enhance the conservation of panel paintings

L. Riparbelli, P. Dionisi-Vici, P. Mazzanti, F. Brémand, J.C. Dupré, M. Fioravanti, G. Goli, T. Helfer, F. Hesser, D. Jullien, et al.

Journal of Cultural Heritage – Elsevier

To cite:
L. Riparbelli, P. Dionisi-Vici, P. Mazzanti, F. Brémand, J.C. Dupré, M. Fioravanti, G. Goli, T. Helfer, F. Hesser, D. Jullien, P. Mandron, E. Ravaud, M. Togni, L. Uzielli, E. Badel, J. Gril,
Coupling numerical and experimental methods to characterise the mechanical behaviour of the Mona Lisa: a method to enhance the conservation of panel paintings, Journal of Cultural Heritage, Volume 62, 2023, Pages 376-386, ISSN 1296-2074, https://doi.org/10.1016/j.culher.2023.06.013.

Coupling numerical and experimental methods to characterise the mechanical behaviour of the Mona Lisa: a method to enhance the conservation of panel paintings

L. Riparbelli[1], P. Dionisi-Vici[1], P. Mazzanti[1*], F. Brémand[2], J.C. Dupré[2], M. Fioravanti[1], G. Goli[1], T. Helfer[3]. F. Hesser[2], D. Jullien[4], P. Mandron[5], E. Ravaud[6], M. Togni[1], L. Uzielli[1], E. Badel[7], J. Gril[7,8]

[1] DAGRI, Università di Firenze, Florence, Italy
[2] Institut Pprime, Université de Poitiers, CNRS, Poitiers, France
[3] CEA, DES, IRESNE, DEC, Cadarache F-13108 Saint-Paul-Lez-Durance, France
[4] LMGC, Univ. Montpellier, CNRS, Montpellier, France
[5] Ateliers d'Enghien, 12 rue d'Enghien 75010 Paris, France
[6] C2RMF, Paris, France
[7] Université Clermont Auvergne, INRAE, PIAF, Clermont-Ferrand, France
[8] Université Clermont Auvergne, CNRS, Institut Pascal, Clermont-Ferrand, France
[*] Corresponding author. Email: paola.mazzanti@unifi.it

Highlights

- Integrating innovative numerical analysis and non-invasive experimental tests
- Numerical tool to optimize the conservation conditions of *Mona Lisa*'s wooden panel
- Analysing the internal stress state, and its safe limits, of the panel painting
- FEM numerical modelling for the mechanical characterisation of the artwork
- Assessment of the conservation *status* of panel paintings

Keywords: *Mona Lisa*, FEM modelling, numerical simulation, conservation of panel paintings, non-invasive experimental measurements.

Abstract

A numerical FEM (Finite Element Method) model was implemented to represent the mechanical state of the wooden panel of the *Mona Lisa*, as it is conserved in its exhibition case, and constrained in its auxiliary frame. The model is based on the integration of advanced numerical analysis and various experimental examinations carried out non-invasively on the artwork by the authors during over 15 years. This includes visual, microscopic and X-ray observations together with mechanical measurements and monitoring of panel deformations and constraining external forces. In addition to the development of non-invasive techniques to characterise the mechanical properties of the panel, the FEM model reliably evaluated the

strains and stresses generated in the panel by the various actions it experiences. The paper consists of the following parts: (i) a short summary of the experimental measurements and other observations, (ii) a detailed description of the FEM numerical model, of the hypotheses it is based on, and of its advantages and limits, (iii) the main results obtained by running the model. This includes the identification of local strains and stresses, the location of most critical areas, an evaluation of the risk that the existing ancient crack may propagate, and an evaluation of safe ranges for the forces acting on the wooden panel, (iv) the validation criteria for such results, and (v) a discussion about the significance of the mechanical model.

1. Introduction

The conservation of panel paintings is a topic that researchers from various fields have dealt with for the last 70 years, at least, from different points of view. Some have investigated the hygro-mechanical behaviour of the main materials making up such artwork, tested on new materials [1-5], others the hygro-mechanical behaviour of mock-ups tested in the laboratory [6-10] and some others numerical modelling based on mock-up behaviour or literature data to interpret their behaviour [11, 12-14]. The present research rather focuses on an authentic artwork, as already proposed by [15-20], following the consideration that each panel painting shows a specific hygro-mechanical behaviour which should be known for its preventive and remedial conservation, as highlighted both by testing and numerical modelling in [21,22]. Since 2004, the wooden panel on which Leonardo da Vinci painted his *Mona Lisa* has been studied by an international research team under the request of the curators of the Louvre Museum. Several experimental campaigns have been carried out to observe, measure, monitor and understand its mechanical, hygroscopic and shape characteristics and behaviour, to evaluate its present state of conservation, and to provide related suggestions [23].

The work of the international research team was mainly developed around the following interrelated topics:

i. studying the artwork by direct observation and measurements (typically once a year, during the few hours when the *Mona Lisa* panel is out of its climate-controlled display case, for the routine inspection of its conservation conditions, or for the execution of specific studies or measurements) [23];
ii. monitoring the mechanical behaviour (namely forces and deformations) of the panel in the exhibition case, by special ad-hoc equipment, conceived and implemented specifically for this task [23];
iii. developing, calibrating and validating numerical models based on the first two points observations, to characterise, reproduce and deeply understand the original artwork's behaviour, as consequence of external hygroscopic and/or mechanical actions that might (actually or hypothetically) occur.

The third topic, namely the development of an innovative numerical model, is the main subject of this paper. The two first topics will also be recalled in the following, since they are an indispensable basis for understanding.

The methodological approach we propose for the numerical analysis of a real panel painting takes into account the following directly observed characteristics in order to reflect the actual behaviour of the artwork:

- analysis of the construction techniques of the artwork, characteristic of the period, school and workshop in which it was assembled;
- knowledge of the current conservation techniques and methods;
- assessment of the actual shape of the panel;

- technological study of the panel: identification of the wood species and the cutting pattern of the board;
- observation of the damages (such as the crack) that occurred in the past and their consequences on the artwork;
- study of the dynamics of contact between the artwork and any stiffening elements such as frames and crossbeams;
- study of the reaction of the panel to applied forces and solicitations in general.

A fundamental aspect is the importance of the mechanical characterisation of an artwork. However, destructive or invasive tests are unacceptable. Thus, non-invasive methods are required to mechanically characterise the different components such as the wood and the ground and paint layers.

In this paper, the numerical analysis is limited to the mechanics of the panel to answer the question of its current state of conservation. The study of the hygro-mechanical behaviour of the artwork will be discussed in a future publication. Previously published work [23-27] confirmed the relevance of integrating computational tools with experimental data directly obtained from the original artwork being studied. This approach, which has been gaining ground in recent years [20-22,28], has necessarily required collaboration among scientists, conservators and restorers, and can be considered as an important step towards fully integrating this kind of research for the in-depth knowledge and conservation of the physical structure of the wooden artwork.

Starting from such approach, the considerable difficulties found in fully interpreting the results of the experimental observations and measurements have highlighted the complexity of the phenomena observed, and the variability from case to case of the observed behaviours. On the one hand, these difficulties have confirmed the uniqueness (i.e. non-generalizability) of each artwork also from the material and behavioural viewpoints (21). On the other hand, it appears that this complexity can be optimally addressed not in a preconceived way, but rather by integrating in an innovative way (as in this paper) the experimental results and adequate computational tools.

2. Aims

This paper describes an innovative method developed in the framework of a project lasting for over 15 years, originated by the curators of the Louvre Museum, aiming to improve the knowledge and optimize the conservation conditions of the *Mona Lisa* wooden panel.

The method is based on the integration between advanced numerical analysis and several experimental examinations carried out non-invasively on the artwork during the project. This paper briefly summarises such examinations, provides details of the numerical model, its validation by means of the experimental data, and its actual or potential developments. The main aims are a) to provide a tool capable to characterise a real panel painting and b) to evaluate the internal stress state of the wooden support, and its safe ranges, deriving from applied forces (or climatic variations, when the hygro-mechanical model will be discussed); so that well-motivated decisions for optimizing its conservation conditions can be made.

Among other beneficial outcomes, the numerical model has already provided valuable technical guidelines for the design of a mechanism (recently implemented in the *Mona Lisa*'s auxiliary frame) to automatically limit the forces acting on the wooden support within safe ranges.

3. Materials and methods

In this section, all the specificities of a real panel painting are analysed, specifically by observing and measuring them directly, in a non-invasive manner, associating them with the numerical modelling tools.

3.1 Short recall of *Mona Lisa*'s wooden structure and measurement equipment

The *Mona Lisa*, painted approximately in the years 1503-1506, is almost unaltered and well preserved despite the several accidents that occurred to it throughout its centuries-old existence [24]. The paint layers are applied on the "external" face (that is, the face away from the pith of the trunk from which the board was obtained) of a flat-sawn poplar (*Populus alba* L.) panel, measuring 794 x 534 x13 mm. The panel is curved both longitudinally and transversally, with the convexity towards the front face. It is pressed against the rim (*feuillure*) of the intermediate auxiliary frame (*châssis-cadre*) by two crossbars screwed onto the auxiliary frame itself. The auxiliary frame, with the panel inside, is in turn hosted and pressed by metal brackets in a carved and gilded external wooden frame. An ancient radial-longitudinal crack runs through the wood thickness from the top edge of the panel down to the Lady's forehead. Two wooden "butterflies" have been inlaid, possibly during the 19th century, into the panel's thickness to prevent any longitudinal propagation of the crack, one of them now missing and being replaced by a glued canvas strip.

The *Mona Lisa* was equipped to monitor both the deformations that the panel undergoes (mainly produced by the inevitable small climatic fluctuations within the display case) and the constraining forces acting on the panel itself. Such equipment includes load cells hosted in the top and bottom crossbeams and further instrumentation (transducers, data-logger, and various electronics) housed in a closed and robust aluminium case fixed on the auxiliary frame at mid-height, facing but not touching the back of the panel. Case and crossbeams were re-designed and replaced several times according to the evolution of the instrumentation, and the measurement methods are in-depth described in [23].

3.2 Optical measurements

The shape to be used to create the geometrical model was determined by the method of fringe pattern profilometry. This technique [29,30] consists in projecting a series of parallel lines on the panel, recording the fringes by a camera and analysing how the panel deforms the fringes. An ad-hoc developed method permits to obtain accurate measurements, with an accuracy of nearly 0.03 mm for a resolution of 0.45 mm/pixel. From this method, two point clouds have been created, which are the front and the back of the panel. As both were elaborated in the same reference system, it was possible to reconstruct the whole 3D shape, including the varying thickness. The generated shape is taken with the panel not subjected to external forces.

3.3 Force and displacement measurements

To produce the numerical model, more detailed information was necessary about the mechanical behaviour of the panel. A force-deformation test was performed during an annual inspection day, to observe its elastic behaviour. Since the forces were already measured by four load cells mounted on the ends of the "upper" and "lower" crossbeams [23], a slight variation of forces was produced by screwing or unscrewing the grub screw there inserted. With the lifting, or lowering, of the grub screw and its precise measuring, it is possible to correlate them to the force variations and hence a force-deformation behaviour could be determined. In order to carry out such test, a specific measuring device was designed at DAGRI (University of

Florence), named *Jocondometer* [23]. This made-on-purpose device measures the lifting or lowering of the grub screw that pushes on the load cell in which it is inserted [23].

Before carrying out the tests, two aspects that could affect the reliability of the results were considered : (i) possible contacts between the auxiliary frame and the panel borders; (ii) the mechanical interaction between the panel and the auxiliary frame. The possible contacts between the auxiliary frame and the panel edges were checked all around the panel by inserting a feeler gauge of 0.1 mm and no contacts were observed. The other question was to exclude the mechanical contribution of the auxiliary frame to the test, so it was stiffened by fastening on it a 20 mm thick MDF panel. Finally, the experimental test was carried out through screwing or unscrewing the grub head screw by 0.25 mm on one load cell at a time, while the other three remained unchanged. Each step variation of force was recorded with an acquisition rate of 1 sec [23]. When the test was completed for one measuring point, the load cell was repositioned to the value of the display condition and the same experimental procedure was applied to the other measuring points.

3.4 Contact zones identification

In 2012 a specific campaign described in [31] was made to assess the contact zones and pressures of the front face of the panel when inside the auxiliary frame. The measurements were made using a pressure-sensitive film (Prescale®) made of two strips, one with colour micro-spheres and the other with a developing material. In brief, thanks to the fact that the two films are interposed inside a mechanical coupling, they show a colour map of the contact zones with a red scale indicating point-by-point the scalar value of the pressure, in a non-invasive way. The results showed the presence of three main contact zones, confirming the convexity of the panel toward the front.

3.5 Observation of the anatomy of the panel and its modelling

It is well known that wood exhibits a strongly anisotropic behaviour of mechanical and hygroscopic properties [32-33]. This is always a challenge and an aspect of paramount importance in modelling. Thus, it is of great importance to study the tree orientation of the panel. The localization within the trunk was carried out through an optimization process based on the experimental measurements of the growth rings visible on the edges, the X-ray images and the traces on the back drawn on a melinex sheet. Two variables were associated with this experimental evidence: the possible angle of inclination of the panel with respect to the pith axis and the angle of development of the conical surfaces of the growth rings in the plant height. This geometric optimisation, carried out using the open source 3D modelling software SalomeMeca, developed by Electricité de France [34], made it possible to visually identify a best match for a 4% (2 sexagesimal degrees) inclination of the conical surfaces of the growth rings and a 1% (0.5 sexagesimal degrees) inclination of the panel with respect to the pith axis, i.e. the cutting angle. A value of 8% of the original tree taper was therefore identified, a plausible value for the lower part of a large poplar tree grown in isolation.

To consider the correct anatomical directions of the panel, we decided to represent the elasticity of the solid in a cylindrical reference, proceeding to a point-by-point definition of the compliance matrix based on the cylindrical coordinates centred in the pith of the trunk that generated the panel. For each position a local orthonormal reference system with three axes x1, x2, x3 was defined, corresponding to the radial (R), tangential (T) and longitudinal (L) anatomical directions of wood, respectively. Due to the conicity of the trunk it was related to the cylindrical reference system by a rotation in the RL plane.

The mechanical behaviour of the wooden panel was assumed hereafter to follow an orthotropic elastic behaviour characterised by 9 elastic coefficients, that will be identified by an inverse approach in Section 3.8.

This behaviour has been implemented using the MFront open-source code generator [MFrontA, MFrontB] [35,36] as described in Appendix A.

Thus, each material point of the continuum saw its elasticity, intended as the fourth-order compliance tensor, rotated in the RT plane according to its position with respect to the pith to represent radial and tangential anisotropy, and in the LR plane to represent the conicity of evolution in the vertical direction of the growth rings.

3.6 Geometrical shape and discretization

The surfaces of the front and back have been reconstructed starting from the point clouds inside Rhinocerous 3D [37] and then exported to the open-source 3D modelling platform Salome-Meca, from which the 3D body has been built. Through Boolean operations and partitions the body was enriched with the contact surfaces described in Section 3.4, the fracture and the butterfly described in Section 3.1. After taking into account the observations in Section 3.2, the panel model was placed relative to the origin of the axes; additionally, a body comprising the front part of the *auxiliary frame* was added to the model. In the geometric model, a surface pictorial layer of 0.2 mm was considered to represent the ground layer of the *Mona Lisa*, such value being an approximation obtained from direct observation. To such surface layer, specific mechanical characteristics were added, different from the wood.

The numerical model was built by meshing this body with a Netgen algorithm, computed within Salome-Meca. The following criteria were adopted for the construction of the mesh:

- Maximum Aspect Ratio: 5
- Minimum Angle: 4 degrees
- Maximum Warping: 4 degrees
- Minimum Transition Factor: 0.4

Additionally, refinements of the discretization were required for the internal surfaces of the fracture, for the contact surfaces between the butterfly and the panel painting, for the auxiliary frame and the panel painting contact areas, and finally for the areas that showed accentuated curvatures such as the edges or imperfections of the back.

The mesh was refined close to the contact zones with the load cells at the back. The resulting mesh was composed of 441999 second-order 10 nodes-tetrahedrons (Figure 1).

The ground and paint layers were modelled with two-dimensional elements, in accordance with the Kirchhoff-Love theory, that share their nodes with the nodes of the wood surface elements, with an eccentricity of the half of the thickness to avoid a physical overlap. The thickness used in the model for these surface elements was 0.2 mm, that describes all layers of the coating in one surface element. This parameter is very uncertain and variable inside an artwork, however, in the *Mona Lisa* it was observed that it is thin and made only of *blanc de plomb*. The modelling choice for the ground and paint layers was therefore to consider them as a single layer with homogeneous mechanical characteristics and in the overall mechanical relationship with the wooden support as a composite with perfect adherence of the two surfaces. In the following, they will be simply designated as “paint”.

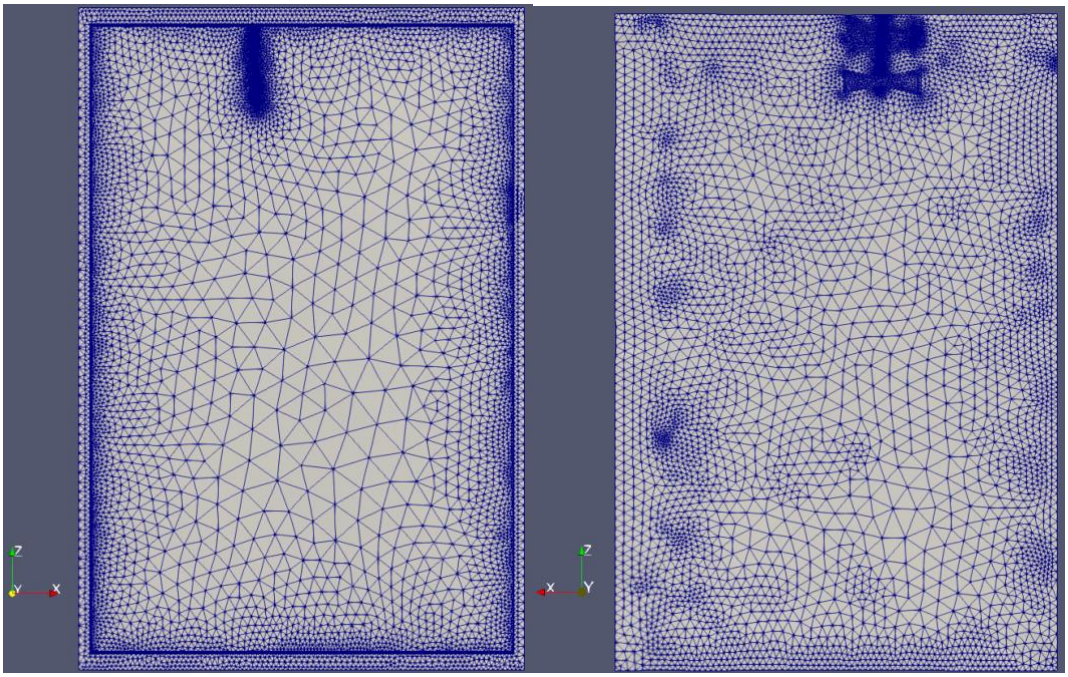

Fig. 1. Geometrical discretization of the wooden panel. The refinement of the mesh was increased in the zones that show spatial particularities.

3.7 Nonlinear analysis with contact mechanics

Finite element analyses were performed with the opensource solver code_aster, developed by EDF [34]. This tool was used for its high level of industrial validation, the quality of the algorithms in case of mechanical contacts, the possibility to run in parallel allowing to solve large problems in a reasonable time, and above all the fact that it works as a low-level programming language allowing integrating directly blocks of code and custom algorithms. Moreover, the opensource licence ensures transparency and replicability of the numerical methods.

To consider the correct behaviour of the panel with the auxiliary frame in which it is inserted, it was decided to carry out analyses that consider nonlinear contact, with friction.

The numerical treatment of the contact-friction phenomenon was dealt with a Stabilized Lagrangian formulation [38] following Signorini-Coulomb law. From the operational point of view, two surfaces are defined in correspondence of the contact zone, commonly called master and slave; to enforce the contact condition means to prevent the slave nodes to penetrate the master surfaces. In the light of this assumption, in order to ensure a solid and rapid convergence of the non-linear solution, the following logic was considered for the choice of contact surfaces [39]: the one that presented the lower rigidity in the direction normal to contact, the one with the lower area, or the one with a less fine mesh compared to the other, was chosen as the slave surface between the two in contact (result in Figure 2). The contact areas detected by the pressure sensitive film (Section 3.4) were then inserted as slave contact areas, leaving the upper edge of the auxiliary frame as the master surface.

In all the simulations the following simplifications were assumed: the panel not subjected to external forces does not present stresses and strains; all the materials are homogeneous; their characteristics are not moisture dependent.

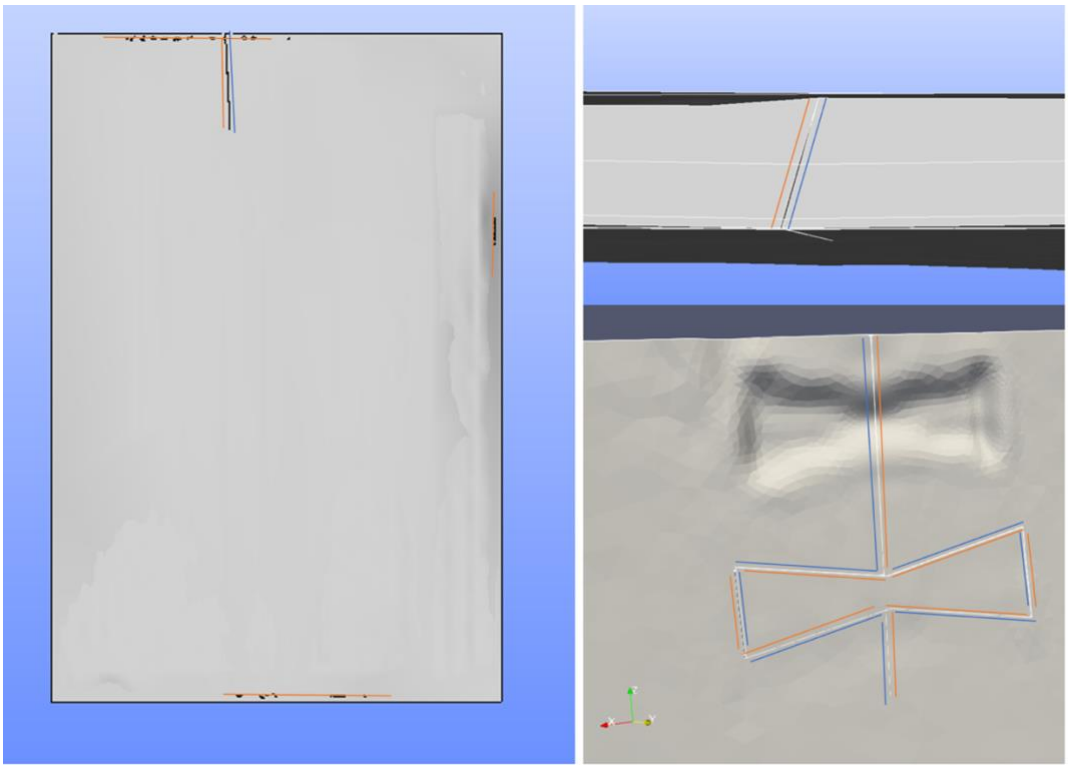

Fig. 2. Contact zones: in red the slave surfaces, in blue the master surfaces.

3.8 The optimization scheme

To determine the mechanical characteristics of the panel and the paint, an iterative optimization technique was used. A cost functional *J* was introduced, dependent on c, vector of the n parameters to be identified:

$$J(c) = \|d - d_{exp}\| \tag{1}$$

where d are the numerically calculated reactions in the position of the load cells, d_{exp} are the corresponding mechanical reactions experimentally determined and $\|\cdot\|$ is a norm on L, space of the observable values. The inverse identification is a minimization of the cost functional *J(c)*, where we want to find $c^* \in O$, closed convex of $\mathbb{R}^n$:

$$J(c^*)=\min_{c\in O} J(c) \tag{2}$$

The minimisation was performed by means of a technical solution [40] based on the succession of a genetic algorithm followed by a Nelder Mead-type Click or tap here to enter text. minimisation scheme. This proves to be a very effective method [41] for finding solutions where, in general, a small variation in the coefficients objects of the minimization, generates considerable variations in the results.

The wood part is assumed to behave elastically according to cylindrical orthotropy, with a compliance matrix expressed in the following way:

$$\underline{\underline{S_{ij}^*}} = \begin{pmatrix} aS_{11}^0 & \sqrt{ab}S_{12}^0 & \sqrt{ac}S_{13}^0 & 0 & 0 & 0 \\ \sqrt{ab}S_{12}^0 & bS_{22}^0 & \sqrt{bc}S_{23}^0 & 0 & 0 & 0 \\ \sqrt{ac}S_{13}^0 & \sqrt{bc}S_{23}^0 & cS_{33}^0 & 0 & 0 & 0 \\ 0 & 0 & 0 & \sqrt{bc}S_{44}^0 & 0 & 0 \\ 0 & 0 & 0 & 0 & \sqrt{ac}S_{55}^0 & 0 \\ 0 & 0 & 0 & 0 & 0 & \sqrt{ab}S_{66}^0 \end{pmatrix} \tag{3}$$

where $\underline{\underline{S_{ij}^*}}$ is the optimized compliance tensor, S_{ij}^0 the components of the compliance matrix estimated based on the actual mean density of around 450 kg/m^3 [43], and *a,b,c* are constant coefficients affected by the optimization. The paint behaves according to isotropic elasticity, with a Young's modulus E_P= *d* GPa, where *d* is coefficient also subjected to optimization, and a Poisson's ration ν_P set to a fixed value of 0.2.

For the sensitivity analysis, the variance-based Sobol method was used as it can handle non-additive, non-monotonic and non-linear systems, following the same schema of [22]. In a Sobol sensitivity analysis, the first-order index and total index are commonly used to measure the sensitivity of a model output to input parameters. The first-order index assesses the fractional contribution of an individual input parameter to the overall variance of the model output, without considering any interaction effect with other input parameters. It measures the individual importance of a single input parameter and can be used to rank input parameters in terms of their relative importance. The total index takes into account the effects of interactions between input parameters, including their first-order effects and all higher-order interactions. It provides a more comprehensive measurement of the impact of an input parameter on the model output. Both indexes are needed to identify the most important input parameters and provide insights into the overall behaviour of the model. The results obtained show the significance of the chosen variables; the results being qualitatively very similar for the four positions, we present in Figure 3 only the values of first order and total index related to position 1. The fact that the first-order index and total index are very near, means that the individual input parameter has a dominant effect on the model output, and the higher-order interactions between this parameter and other parameters are relatively weak or negligible. In other words, the interaction effects are not significant enough to alter the contribution of the individual parameter significantly. The study utilized the open-source software Persalys [42] for handling uncertainties and variability. This software is based on the extensively validated openTurns methods [43] and can be seamlessly integrated with code_aster. This integration enabled efficient and rigorous investigations of sensitivity on the finite element model.

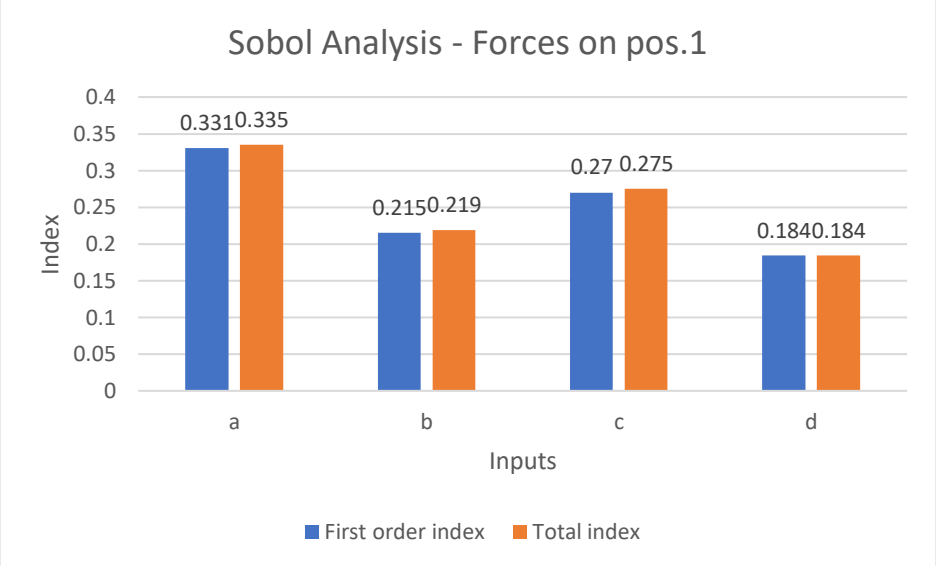

Fig. 3. Sobol sensitivity analysis results for the force generated by an imposed displacement of 0.25 on the position 1

4. Model fitting and validation

The iterative optimization process led to identify the values of wood rigidity in anatomical directions (L, R, T) and that of the paint layers (Table 1), for a reference temperature of 25°C, since the climatic conditions in the room during the test were 25°C and 53 % RH..

Table 1. Initial and optimized value of rigidities.

Rigidity	Initial values	Optimized values
$E_L = \frac{1}{S_{11}^0}$	10.06 [GPa]	9.60 [GPa]
$E_R = \frac{1}{S_{22}^0}$	1.19 [GPa]	1.02 [GPa]
$E_T = \frac{1}{S_{33}^0}$	0.58 [GPa]	0.73 [GPa]
$\frac{E_L}{\nu_{LR}} = \frac{E_R}{\nu_{RL}} = \frac{1}{S_{12}^0}$	28.25 [GPa]	31.33 [GPa]
$\frac{E_T}{\nu_{TL}} = \frac{E_L}{\nu_{LT}} = \frac{1}{S_{13}^0}$	21.40 [GPa]	19.70 [GPa]
$\frac{E_R}{\nu_{RT}} = \frac{E_T}{\nu_{TR}} = \frac{1}{S_{13}^0}$	1.69 [GPa]	1.76 [GPa]
$G_{RT} = \frac{1}{S_{44}^0}$	0.2 [GPa]	0.21 [GPa]
$G_{LR} = \frac{1}{S_{55}^0}$	0.64 [GPa]	0.59 [GPa]
$G_{LR} = \frac{1}{S_{66}^0}$	0.86 [GPa]	0.95 [GPa]
E_{GROUND}	1.0 [GPa]	1.96 [GPa]
ν_{GROUND}	0.2	Not subjected to optimization

For the paint an isotropic Young modulus of 1.96 GPa was identified, a value consistent with data for gypsum [44].

A process of evaluation of these results was established to ensure the consistency of the numerical model with the experimental observations.

Table 2 shows the reactions generated on each load cell for an increment of vertical displacement of 0.25 mm (Section 3.3). A good matching was obtained between the experimental reading and the numerical result of the numerical model, with a notable difference only for L8.

For an estimation of the level of uncertainty, we considered a radius error equal to the difference between the experimental and numerical results of each cell and calculated all combinations of the values of a, b, c, and d that generate force values falling within these ranges. We decided to proceed in this way considering the fact that the individual areas of the painting exhibit significantly different physical behaviours. Technically, the calculation was performed using the Persalys software, based on the Openturns library, coupled with Code_Aster. Wide intervals of uniform variation (0.5-1.5) were defined for the variables a, b, c, and d, and a Monte Carlo-type algorithm was used to construct 1000 combinations for each of the four load cases. From

each of these 1000 computations, those whose force value was within the error range for each cell were extracted, and the extremes for the variables a, b, c, and d were extracted as reported in Table 3.

Table 2. Measured forces on the back of the panel for a given displacement (Section 3.3), and corresponding calculated values.

Load Cell	Experimental values [N]	Numerical values [N]	Difference [N]
L1	8.58	8.61	0.03
L2	5.37	5.49	0.02
L7	6.46	6.42	-0.04
L8	7.94	7.53	-0.41

Table 3. Range of variation of each optimization coefficient associated to the maximum error between experimental and numerical results.

Load Cell	Force variation [N]	a	b	c	d
L1	8.58±0.03	[1.04 ÷ 1.06]	[1.15 ÷ 1.17]	[0.78 ÷ 0.81]	[1.92 ÷ 2.02]
L2	5.37±0.02	[1.05 ÷ 1.06]	[1.16 ÷ 1.17]	[0.78 ÷ 0.8]	[1.93 ÷ 1.99]
L7	6.46±0.04	[1.04 ÷ 1.06]	[1.14 ÷ 1.18]	[0.78 ÷ 0.82]	[1.91 ÷ 2.04]
L8	7.94±0.41	[0.92 ÷ 1.18]	[0.95 ÷ 1.37]	[0.71 ÷ 0.96]	[1.65 ÷ 2.32]

This study highlights how the variation ranges of the optimized parameters in positions 1, 2, and 7 are uniform and reasonably tight, while for position 8, the values are more uncertain. The reason for this could be a non-uniformity in one or more materials in that area, a slight deviation in the wood grain, wood variability or an experimental discrepancy related to that position.

The validation of the predictive model was done by comparing measured and calculated displacements perpendicular to the plane of the panel. For an increment of force of 5 N on the load cell L2, the vertical displacement in the transducer T3 was measured and computed, then the process was repeated applying the same increment in L8 and reading the displacement again in T3. Figure 4 shows the results of this procedure with a good matching.

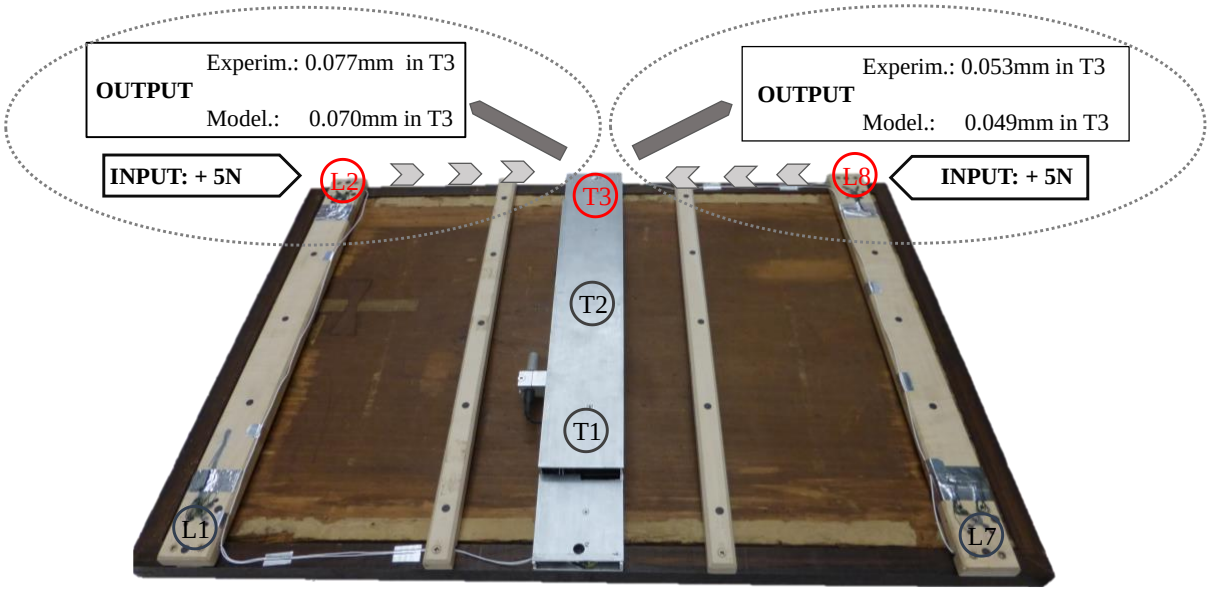

Fig. 4. The process to validate the predictive model and the results. A variation of force (+ 5N) was applied on L2 during an experimental test on the *Mona Lisa* and the consequent displacement was measured in T3 resulting in 0.077mm; then the displacement was computed by means of the numerical model resulting in 0.070 mm when the same force variation was applied. The same process was applied in L8, which produced a measured displacement of 0.053mm in T3 and computed of 0.049mm. The slight difference between the experimental data and the model output indicates the goodness-of-fit of the numerical model.

A further evaluation of the accuracy of the model was carried out from optical measurements. However, the comparison can only be made qualitatively, considering that the deformations obtained are conditioned by an albeit slight deformability of the contact zones due to the bending and torsional distortion of the *auxiliary frame*. The effect of this difference is easily seen in the lateral contact areas: while in the model they are at a constant and equal height to the other contacts, in the optical shots they change their mutual height depending on the stiffness of the *auxiliary frame*.

The four cases shown in Figure 5 represent four different boundary conditions applied on the panel. Despite the limitations of the comparison discussed above, we can see that the behaviour of the panel is extremely close between optical imaging and numerical modelling. Again, it allows us to consider the model to approximate closely the physical reality of the *Mona Lisa* support.

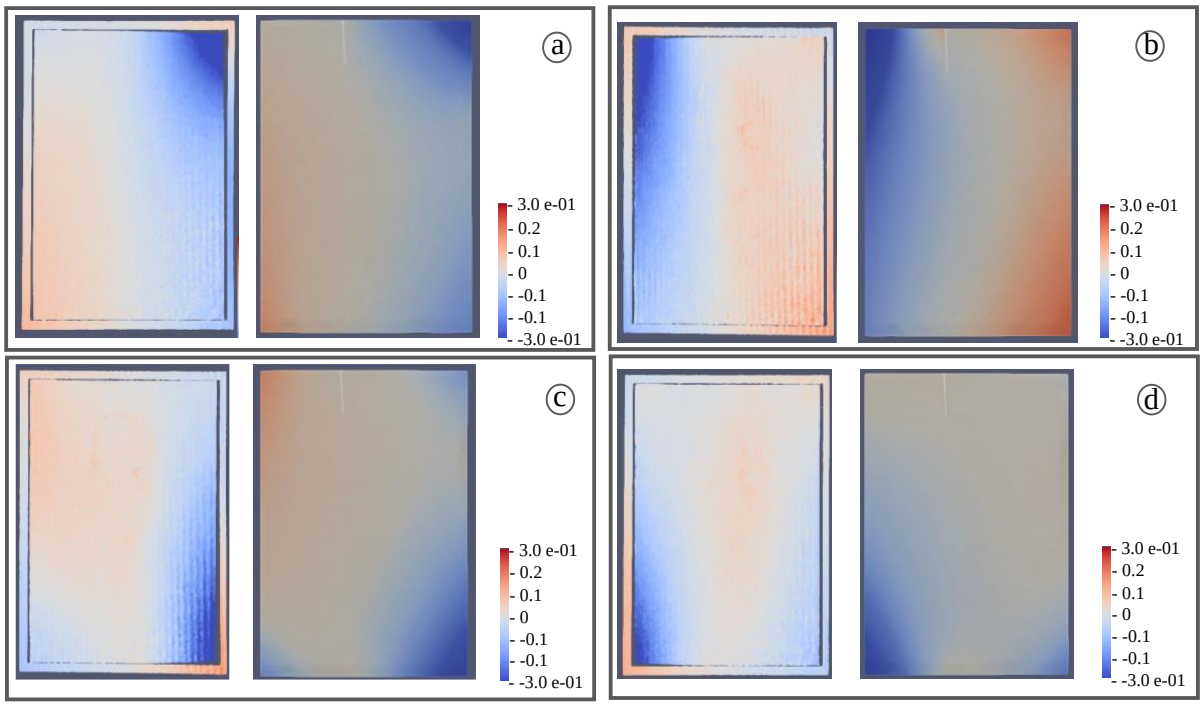

Fig. 5. Comparison between optical measurements (on the left of each black box) and numerical model (on the right of each black box). For each couple of images, the out-of-plane displacement [mm] is displayed, on the left the optical measurement and on the right the numerical model. The images are front view; thus, the auxiliary frame is clearly visible on the optical measurements. Four cases are presented characterised by specific boundary conditions, a load decrease of 9.48 N for position 1 (a), 5.54 N for position 2 (b), 8.17 N for position 7 (c), 7.48 N for position 8 (d), respectively.

5. Discussion

The model presented in this study does not consider the hygroscopic and moisture-dependent behaviour of the panel, but despite this, as the climatized display case of the *Mona Lisa* at the Louvre Museum keeps the humidity and temperature values extremely constant, it can be used to understand directly the tensional and deformation states of the panel painting in its standard conservation conditions.

A panel left free of stiffening tends to develop a permanent curvature toward the painted face due to the hygroscopic oscillations of its storage environment; this phenomenon is known in the wood science sector as compression set [5,45]. To avoid permanent deformations typically induced by compression set phenomena, forces are normally applied to the panel by the restraining system, in our case the *auxiliary frame*. Such forces are considered as the boundary conditions for the numerical model presented in this Section (Table 4).

Table 4. The forces applied by the restraining system to the *Mona Lisa* measured by the load cells.

Location	L1	L2	L7	L8
Measured forces [N]	7	15	17	11

A first level of results to be discussed are the main directions of deformation at the interface between wood and paint. In Figure 6 the principal deformations of the painted side of the panel are shown. They represent the directions in which the wood is subjected to simple contraction or extension, and no shear strain; the deformations have extremal values in these directions. Due to the assumption of perfect adherence between paint and wood, their deformation is

expected to be identical at their interface; the same cannot be said for stresses, related to the deformations through different constitutive models (isotropic pictorial layers, orthotropic wood) resulting in different in-plane stiffnesses [46].

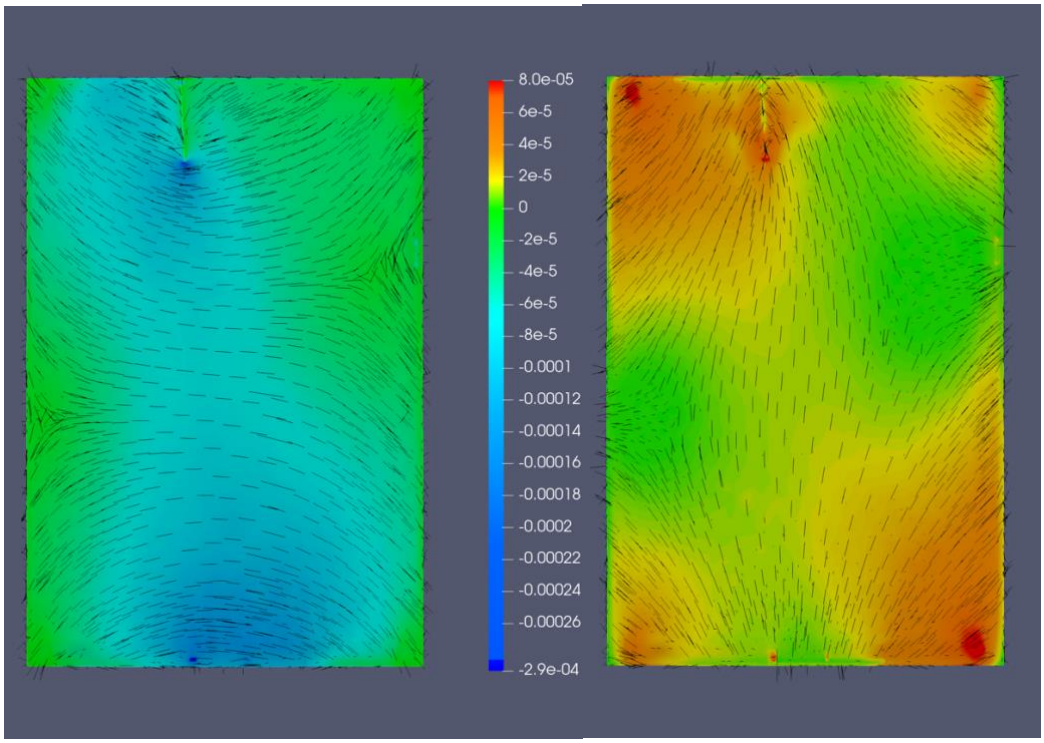

Fig. 6. Principal simulated strains directions and related values at the interface between wood and pictorial layers. In blue the contraction strains, in red the extension strains.

The deformation values are much lower than those identified in the literature [47] for the damage of the ground layer, confirming the efficiency of the current conservation method at the Louvre Museum.

In Figure 7, the main stresses to which the panel painting is subjected in its display condition can be observed. The tensile stresses perpendicular to the grain are generally low, calculated between 0 and 0.15 MPa, even if concentrations occur immediately below the fracture, where the stress increases up to 0.29 MPa (but in the direction of the grain). The compression stresses perpendicular to the grain are very low, as well, calculated between 0 and - 0.15 MPa, up to-0.3 MPa on the underside near the contact zones between the panel and the auxiliary frame. The transverse strength of Poplar wood reported in [4] amounts to 2.56 to 5.14 MP, one order of magnitude higher than those found in the typical display condition of the *Mona Lisa*. Therefore, while the forces and corresponding stresses applied by the restraining system are sufficient to prevent compression set effects, they remain significantly below the threshold of wood strength as a result of panel bending. In other words the panel is maintained in safe stress conditions while being prevented from excessive curvature.

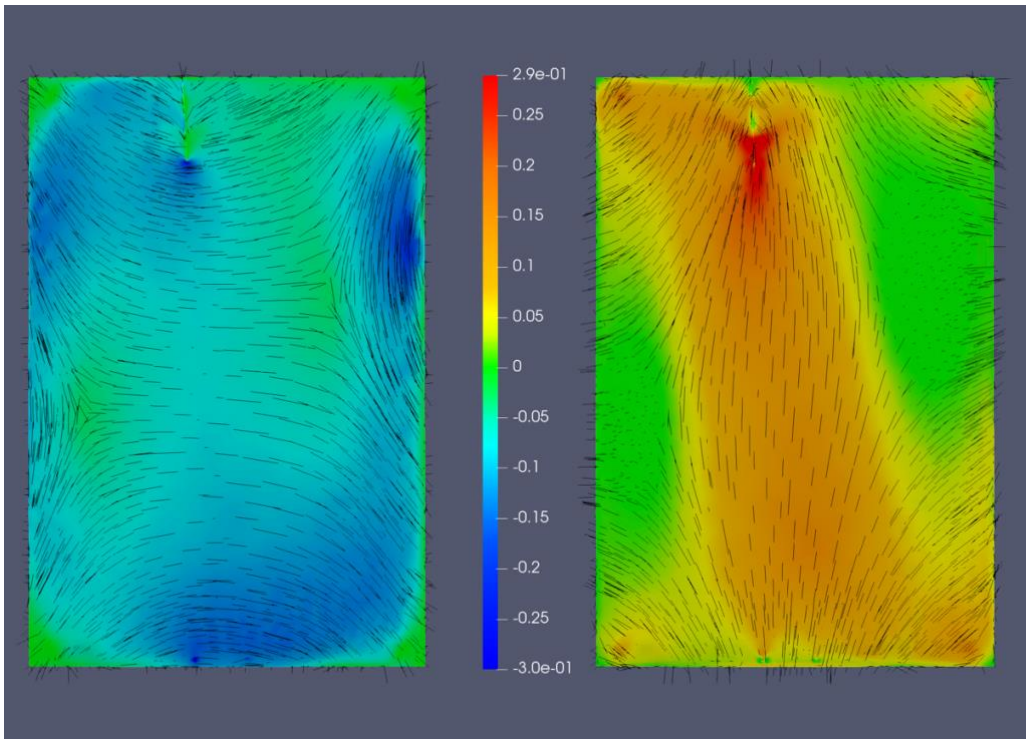

Fig. 7. Main stresses [MPa] calculated in the plane of the panel, extracted in the wood below the paint. On the left are the compression stresses and on the right the tensile stresses. The maximum compression values are localized on the contact area between the panel and the auxiliary frame and the maximum tension stresses are localized near the fracture.

The values showed in Figure 7 are close to 10 % of the transversal wood strength [4], while 20 % is considered as a threshold between the viscoelastic and viscoplastic behaviour of the wood in compression [48,49] and perpendicular to the grain [4]; it is important that our result is in a ratio of 0.5 with the threshold because internal coactions due to non-linear behaviour like mechanosorption, aging, viscoelastic behaviour and damage from the past are not taken into account. It ensures that in the current display conditions no long-term permanent deformations due to mechanical bending occur [23]. Moreover, it prevents from damage from transitory loading over the viscoplastic threshold.

Subsequently, the volumetric density of elastic energy resulting from application of the forces given by Table 4, present in the panel painting under its usual display condition, was calculated both for the wood and the paint (Figure 7). The release of elastic energy being required for the propagation of a crack in quasi-brittle materials such as wood or gesso, its concentration is an indicator of fracture risk. The high concentration in the lower part of the wood can be explained by the concomitance of bending moment and normal contact forces, while the upper part is characterised by a concentration near the fracture only (Figure 8 top left). The deformations being the same at the interface between wood and paint, the difference observed in Figure 8 (top right) is mainly due to the difference in stiffness between the two materials.

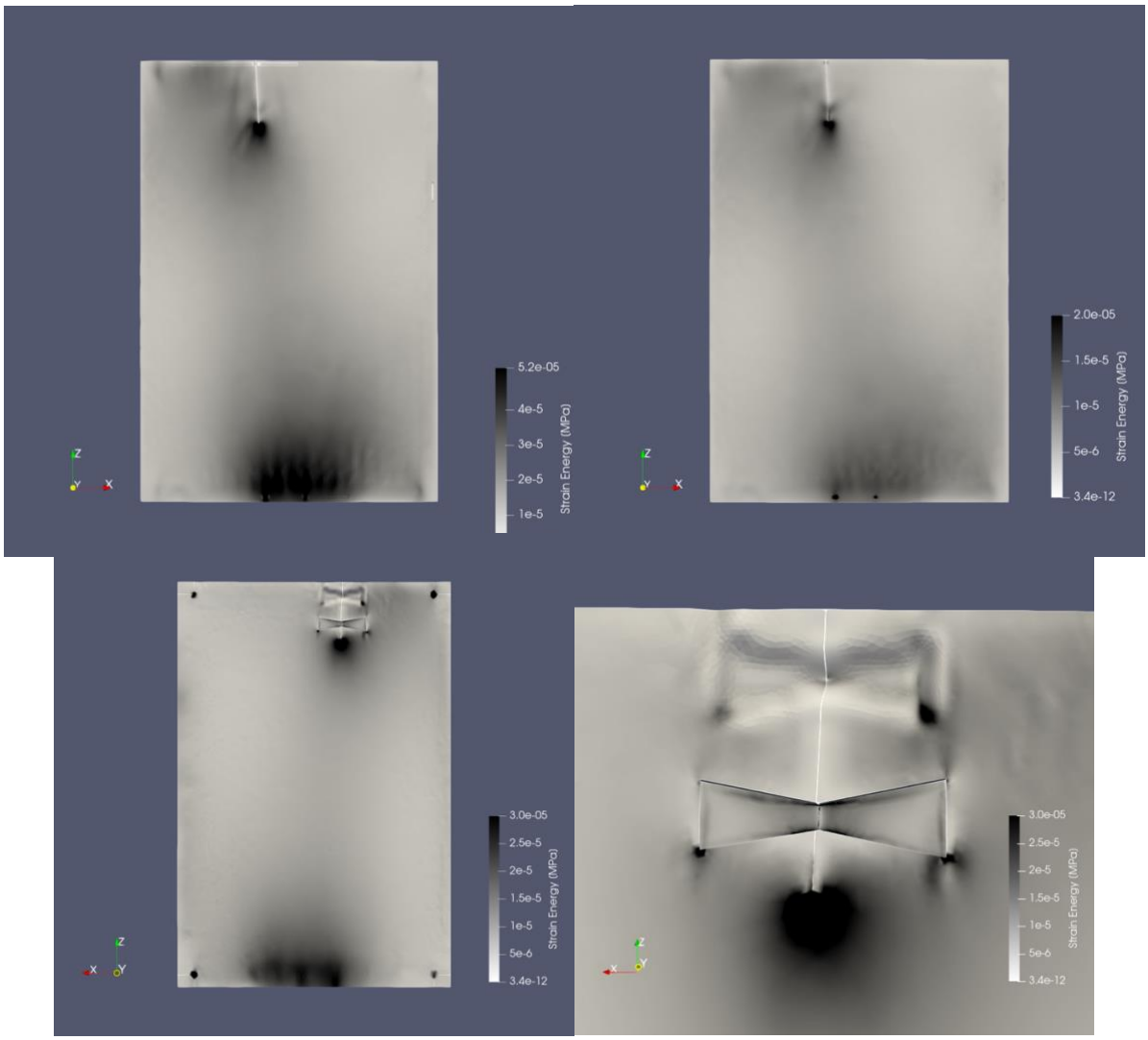

Fig. 8. Volumetric density of elastic energy at the surface of the panel: (a) in the paint (top right); (b) in the wood on the painted side; (c) in the wood, back of the panel; (d) in the zone of the butterfly.

In general, the same operating logic also applies to the reverse side where, in addition (Figure), peaks can be seen in the specific zones of the butterflies, both the one missing and the one present. Taking a closer look at Figure 8, regarding the butterfly, one can observe a trace on the slot just above its tip due to its mechanical effect.

This model was used to calculate the difference in elastic energy between the reference configuration (display condition) and other possible configurations obtained by adding up 5 N on one of each 4 locations of application of the forces at a time. It allowed to evaluate the zones of influence for each point of force application and to determine which have the greatest impact on the overall deformation behaviour of the panel painting, with reference to the fracture (Figure 9).

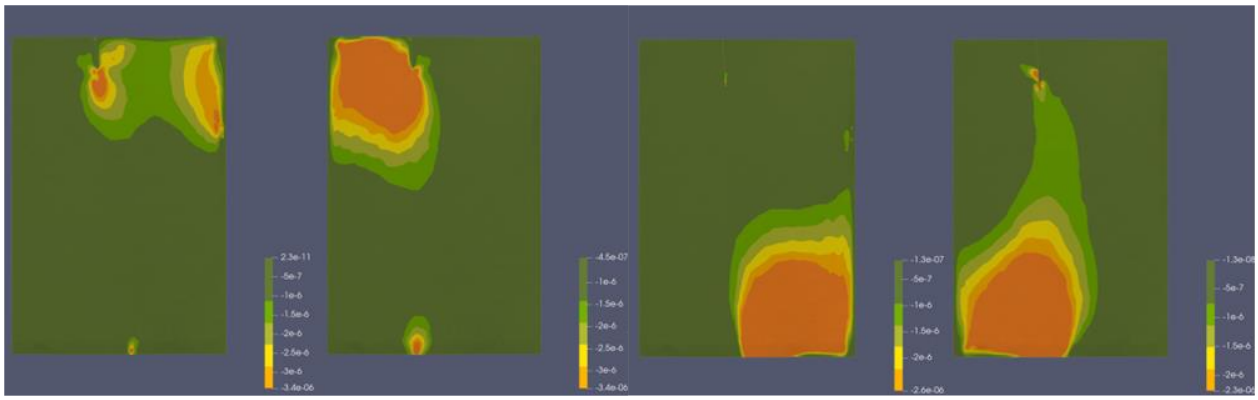

Fig. 9. The difference in elastic energy between the reference configuration (display condition) and other possible configurations obtained by adding up 5 N on one of each 4 locations of application of the forces. From left to right +5 N were applied on L1, L2, L7 and L8 location, from the front.

The behaviour of the panel is essentially independent in its two vertical halves, due to the fracture and the distribution of the contacts. location 2 is undoubtedly the most influential area with respect to the energy embedded in the fracture zone. In this regard, it can be observed that a substantial part of the energy of location 1 is discharged on a lateral contact privileged in terms of force transmission by being aligned in the longitudinal direction of the wood with respect to the point of application of the forces. Finally, location 8, although it mainly affects the lower part of the panel painting (as location 7) showed the greatest global value, even affecting the area close to the fracture.

6. Conclusions

With a sophisticated coupling between a systematic experimental study of the panel of the *Mona Lisa*, and a complex numerical procedure, it was possible to estimate the actual mechanical characteristics of the panel. This numerical model cannot catch the whole complexity of the real artwork, but it can represent consistently the displacements that the panel exhibit when subjected to external forces. Moreover, the model permits to assess of the stresses and strains that may occur for a change in the loads or in general in boundary conditions.

Underlining the intrinsic limitations of this procedure, which can be briefly schematized in a great dependence of the results on the boundary conditions, on the geometry of the continuum and in general on the modelling choices, as well as the great request of computational resources, this method allows to "ask" directly to the object what are its stiffness characteristics in a non-invasive way and respecting its real boundary conditions.

Declarations

This research did not receive any specific grant from funding agencies in the public, commercial, or not-for-profit sectors.

Author’s contributions and roles

LR conceived the methods implemented and the numerical procedures applied, did every step of the modelling, analysed the models and extracted the conclusions, wrote the paper. LR, PDV, LU, PMaz, JG, GG, MT,ER conceived and developed the experimental investigations. PMaz and LU revised the paper. TH and LR developed the law of behaviour for conical elasticity. FB, JCD and FH did and elaborated the optical measurements. LR, MF and JG discussed in

depth the methodological approach. LR, JG, DJ, MF, EB discussed the modelling specifications. PMan took care of the manipulation of the artwork in the experimentation. LR and JG discussed and analysed the conclusions. JG coordinated and directed the project. All authors discussed the research outcome, as well as developed the manuscript. All authors read and approved the final manuscript.

Supplementary materials

Supplementary material associated with this article can be found, in the online version, at doi:10.1016/j.culher.2023.06.013.

Appendix A: Description of the implementation of the elastic orthotropic behaviour of the wooden panel in MFront.

This appendix describes how the elastic orthotropic behaviour of the wooden panel has been implemented using the open source-code generator MFront co-developed under strict assurance quality constraints by CEA, EDF and Framatome in the context of a numerical platform dedicated to the simulation of the nuclear fuel elements named PLEIADES. MFront is distributed as part of the Salomé-Méca platform and is tightly integrated with code_aster.

Notations used

Symbol	Description
$\underline{\underline{\varepsilon}}$	Total strain in the reference system
$\underline{\underline{\varepsilon}}^{\star}$	Total strain in the material frame
$\underline{\underline{\sigma}}$	Stress in the reference system
$\underline{\underline{\sigma}}^{\star}$	Stress in the material frame
$\underline{\underline{\underline{\underline{\mathbf{C}}}}}$	Stiffness tensor in the reference system
$\underline{\underline{\underline{\underline{\mathbf{C}}}}}^{\star}$	Stiffness tensor in the material frame

In the material frame, the orthotropic elastic behaviour amounts to the following relationship between the total strain $\underline{\underline{\varepsilon}}^{\star}$ and the stress $\underline{\underline{\sigma}}^{\star}$:

$$\underline{\underline{\sigma}}^{\star} = \underline{\underline{\underline{\underline{\mathbf{C}}}}}^{\star} : \underline{\underline{\varepsilon}}^{\star} \tag{4}$$

where $\underline{\underline{\underline{\underline{\mathbf{C}}}}}^{\star}$ denotes the stiffness tensor in the material frame.

Let $\underline{\underline{\underline{\underline{\mathbf{R}}}}}$ the fourth order tensor such that:

$$\begin{cases} \underline{\underline{\varepsilon}} = \underline{\underline{\underline{\underline{\mathbf{R}}}}} : \underline{\underline{\varepsilon}}^{\star} \\ \underline{\underline{\sigma}} = \underline{\underline{\underline{\underline{\mathbf{R}}}}} : \underline{\underline{\sigma}}^{\star} \end{cases} \tag{5}$$

Then, the Constitutive Equation 1 can be rewritten as follows:

$$\underline{\sigma} = \left(\underline{\underline{\mathbf{R}}}\right)^{-1} \cdot \underline{\underline{\mathbf{C}}}^{\star} \cdot \underline{\underline{\mathbf{R}}} : \underline{\varepsilon} \tag{6}$$

or, equivalently:

$$\underline{\sigma} = \underline{\underline{\mathbf{C}}} : \underline{\varepsilon} \tag{7}$$

With

$$\underline{\underline{\mathbf{C}}} = \left(\underline{\underline{\mathbf{R}}}\right)^{-1} \cdot \underline{\underline{\mathbf{C}}}^{\star} \cdot \underline{\underline{\mathbf{R}}} \tag{8}$$

MFront provides the mandatory functions to build the $\underline{\underline{\mathbf{C}}}$ from the two rotation matrices corresponding to composition of the rotation in the cylindrical frame and to material frame.

In a sense, usage of MFront in this paper is mostly a matter of conveniency, as performing those operations in code_aster would have been much more cumbersome. However, usage of MFront paved the way for ongoing works, such as including the effect of moisture.

References

[1] M. Mecklenburg, C. Tumosa, D. Erhardt, Structural response of painted wood surfaces to changes in ambient relative humidity. Paint. Wood Hist. Conserv., The Getty Conservation Institute, Dorge V. and Howlett FC, US, 1998, pp. 464–483.

[2] A. Janas, M.F. Mecklenburg, L. Fuster-López, R. Kozłowski, P. Kékicheff, D. Favier, C.K. Andersen, M. Scharff, Ł. Bratasz, Shrinkage and mechanical properties of drying oil paints, Herit. Sci. 10 (2022) 181, https://doi.org/10.1186/s40494- 022-00814-2.

[3] O. Allegretti, F. Raffaelli, Barrier effect to water vapour of early European painting materials on wood panels, Stud. Conserv. (2008), https://doi.org/ 10.1179/sic.2008.53.3.187.

[4] P. Mazzanti, M. Togni, L. Uzielli, Drying shrinkage and mechanical properties of Poplar wood (Popolus alba L.) across the grain, J. Cult. Herit. 13 (2012) S85–S89.

[5] P. Mazzanti, J. Colmars, J. Gril, D. Hunt, L. Uzielli, A hygro-mechanical analysis of poplar wood along the tangential direction by restrained swelling test, Wood Sci. Technol. 48 (2014) 673–687, https://doi.org/10.1007/s00226-014-0633-4.

[6] O. Allegretti, J. Bontadi, P. Dionisi-Vici, Climate induced deformation of Panel Paintings: experimental observations on interaction between paint layers and thin wooden supports, Int. Conf. Florence Heri-Tech Future Herit. Sci. Technol. (2020) 949.

[7] P. Dionisi-Vici, P. Mazzanti, L. Uzielli, Mechanical response of wooden boards subjected to humidity step variations: climatic chamber measurements and fitted mathematical models, J. Cult. Herit. 7 (2006) 37–48.

[8] M. Łukomski, Painted wood. What makes the paint crack? J. Cult. Herit. 13 (2012) S90–S93, https://doi.org/10.1016/j.culher.2012.01.007.

[9] P. Mazzanti, P. Dionisi-Vici, M. Fioravanti, E. Cardinali, J. Mialhe, M. Togni, L. Uzielli, L. Riparbelli, The medusa parade shield by caravaggio: making its structural replica,

laboratory testing, and numerically modelling their hygro- mechanical distortion behaviour, in: R. Furferi, L. Governi, Y. Volpe, F. Gherardini, K. Seymour (Eds.), Future Herit. Sci. Technol., Springer International Publishing, Cham, 2023, pp. 219–234, https://doi.org/10.1007/978-3-031-17594-7_17.

[10] D. Hunt, L. Uzielli, P. Mazzanti, Strains in gesso on painted wood panels during humidity changes and cupping, J. Cult. Herit. 25 (2017) 163–169.

[11] D. Konopka, C. Gebhardt, M. Kaliske, Numerical modelling of wooden structures, J. Cult. Herit. 27 (2017) S93–S102, https://doi.org/10.1016/j.culher.2015.09.008.

[12] C. Gebhardt, D. Konopka, A. Börner, M. Mäder, M. Kaliske, Hygro-mechanical numerical investigations of a wooden panel painting from "Katharinenaltar" by Lucas Cranach the Elder, J. Cult. Herit. 29 (2018) 1–9.

[13] Ł. Bratasz, M.R. Vaziri Sereshk, Crack saturation as a mechanism of acclimatization of panel paintings to unstable environments, Stud. Conserv. 63 (2018) 22–27, https://doi.org/10.1080/00393630.2018.1504433.

[14] Ł. Bratasz, Allowable microclimatic variations for painted wood, Stud. Conserv. 58 (2013) 65–79, https://doi.org/10.1179/2047058412Y.0000000061.

[15] O. Allegretti, M. Fioravanti, P. Dionisi-Vici, L. Uzielli, The influence of dovetailed cross beams on the dimensional stability of a panel painting from the Middle Ages, Stud. Conserv. 59 (2014) 233–240, https://doi.org/10.1179/ 2047058413Y.0000000095.

[16] L. Cocchi, B. Marcon, G. Goli, P. Mazzanti, C. Castelli, A. Santacesaria, L. Uzielli, Verifying the operation of an elastic crossbar system applied to a panel painting: the Deposition from the Cross by an anonymous artist from Abruzzo, sixteenth century, Stud. Conserv. 62 (2017) 150–161, https://doi.org/10.1080/ 00393630.2015.1137426.

[17] P. Dionisi-Vici, I. Bucciardini, M. Fioravanti, L. Uzielli, Monitoring Climate and Deformation of Panel Paintings in San Marco (Florence) and Other Museums, in: Gril J. (ed) Firenze University Press, Firenze, 2009.

[18] P. Dionis-Vici, M. Formosa, J. Schiro, L. Uzielli, Local deformation reactivity of panel paintings in an environment with random microclimate variations: the Maltese Maestro Alberto's Nativity case-study, in: Braga (PT), 2008.

[19] J.C. Dupre, D. Jullien, L. Uzielli, F. Hesser, L. Riparbelli, C. Gauvin, P. Mazzanti, J. Gril, G. Tournillon, D. Amoroso, P.H. Massieux, P. Stepanoff, M. Bousvarou, Experimental study of the hygromechanical behaviour of a historic painting on wooden panel : devices and measurement techniques, J. Cult. Herit. 46 (2020) 165–175, https://doi.org/10.1016/j.culher.2020.09.003.

[20] L. Riparbelli, C. Castelli, G. Gualdani, L. Ricciardi, A. Santacesaria, L. Uzielli, P. Mazzanti, An innovative method for dimensioning the crossbeams of an original painted panel, based on mechanical testing, and on numerically modelling its distortion tendency, in: R. Furferi, L. Governi, Y. Volpe, F. Gherardini, K. Seymour (Eds.), Future Herit. Sci. Technol., Springer International Publishing, Cham, 2023, pp. 97–112, https://doi.org/10.1007/978-3-031-17594-7_8.

[21] L. Riparbelli, P. Mazzanti, C. Manfriani, L. Uzielli, C. Castelli, G. Gualdani, L. Ricciardi, A. Santacesaria, S. Rossi, M. Fioravanti, Hygromechanical behaviour of wooden panel paintings: classification of their deformation tendencies based on numerical modelling and experimental results, Herit. Sci. 11 (2023) 25, https:// doi.org/10.1186/s40494-022-00843-x.

[22] L. Riparbelli, P. Mazzanti, T. Helfer, C. Manfriani, L. Uzielli, C. Castelli, A. Santacesaria, L. Ricciardi, S. Rossi, J. Gril, M. Fioravanti, Modelling of hygro-

mechanical behaviour of wooden panel paintings: model calibration and artworks characterisation, Herit. Sci. 11 (2023) 126. https://doi.org/10.1186/s40494-023- 00958-9.

[23] L. Uzielli, P. Dionisi-Vici, P. Mazzanti, L. Riparbelli, G. Goli, P. Mandron, M.

Togni, J. Gril, A method to assess the hygro-mechanical behaviour of original panel paintings, through in situ non-invasive continuous monitoring, to improve their conservation: a long-term study on the Mona Lisa, J. Cult. Herit. 58 (2022) 146–155, https://doi.org/10.1016/j.culher.2022.10.002.

[24] N. Volle, G. Aitken, D. Jaunard, B. Lauwick, P. Mandron, J.P. RIOUX, Early restorations to the painting, in: J.P. Mohen, M. Menu, B. Mottin (Eds.), Mona Lisa Paint, Abrams, New York, 2006 18.21.

[25] D. Dureisseix, O. Arnould, Mechanical modeling of the activity of the flexible frame, in: J.P. Mohen, M. Menu, B. Mottin (Eds.), Mona Lisa Paint, Abrams, New York, 2006, pp. 52–53.

[26] E. Ravaud, The complex system of fine cracks, in: J.P. Mohen, M. Menu, B. Mottin (Eds.), Mona Lisa Paint, Abrams, New York, 2006, pp. 38–42.

[27] P. Perré, R. Remond, J. Gril, Simulation of the effects of ambient variations, in: J.P. Mohen, M. Menu, B. Mottin (Eds.), Mona Lisa Paint., Abrams, New York, 2006, pp. 50–51.

[28] B. Marcon, G. Goli, M. Fioravanti, Modelling wooden cultural heritage. The need to consider each artefact as unique as illustrated by the Cannone violin, Herit. Sci. 8 (2020) 24, https://doi.org/10.1186/s40494-020-00368-1.

[29] F. Brémand, P. Doumalin, J.C. Dupré, F. Hesser, V. Valle, Measuring the relief of the panel support without contact, in: J.P. Mohen, M. Menu, B. Mottin (Eds.), Mona Lisa Paint, Abrams, New York, 2006, pp. 43–47.

[30] F. Brémand, M. Cottron, P. Doumalin, J.C. Dupré, A. Germaneau, V. Valle, Mesures en mécanique par méthodes optiques, Tech. Ing. hand (2011). https:// www.techniques-ingenieur.fr/base-documentaire/mesures-analyses-th1/ grandeurs-mecaniques-42407210/mesures-en-mecanique-par-methodes-optiques- r1850/. accessed December 7, 2022.

[31] G. Goli, P. Dionisi Vici, L. Uzielli, Locating contact areas and estimating contact forces between the Mona Lisa wooden panel and its frame, J. Cult. Herit. 15 (2013) 391–402.

[32] Wood handbook—Wood as an engineering material, (2010). https:// www.fpl.fs.fed.us/documnts/fplgtr/fpl_gtr190.pdf.

[33] D. Guitard, Mécanique Du Matériau Bois Et composites, Cepadues-Editions, Toulouse, 1987.

[34] EDF - Électricité De France, Finite element code_aster: analyse des structures et thermo-mécanique pour des etudes et des recherches, (2022).

[35] T. Helfer, B. Michel, J.M. Proix, M. Salvo, J. Sercombe, M. Casella, Introducing the open-source mfront code generator: application to mechanical behaviours and material knowledge management within the PLEIADES fuel element modelling platform, Comput. Math. Appl. 70 (2015) 994–1023, https://doi.org/10.1016/ j.camwa.2015.06.027.

[36] https://thelfer.github.io/tfel/web/index.html, (2022).

[37] https://www.rhino3d.com/mcneel/about/, (2022).

[38] EDF - Électricité De France, Éléments de contact dérivés d'une formulation

hybride continue, (2017) 1–77.

[39] EDF - Électricité De France, Notice d'utilisation du contact, (2013) 1–20.

[40] H. Assimi, A. Jamali, A hybrid algorithm coupling genetic programming and
Nelder–Mead for topology and size optimization of trusses with static and dynamic constraints, Expert Syst. Appl. 95 (2018) 127–141, https://doi.org/10.1016/ j.eswa.2017.11.035.

[41] N.E. Mastorakis, On the solution of ill-conditioned systems of linear and non- linear equations via genetic algorithms (GAs) and Nelder-Mead simplex search, in: Proc. 6th WSEAS Int. Conf. Evol. Comput., World Scientific and Engineering Academy and Society (WSEAS), Stevens Point, Wisconsin, USA, 2005, pp. 29–35.

[42] https://persalys.fr/, (2023).

[43] M. Baudin, A. Dutfoy, B. Iooss, A.L. Popelin, OpenTURNS: an industrial software
for uncertainty quantification in simulation, in: R. Ghanem, D. Higdon, H. Owhadi (Eds.), Handb. Uncertain. Quantif, Springer International Publishing, Cham, 2017, pp. 2001–2038, https://doi.org/10.1007/978-3-319-12385-1_64.

[44] J. Sanahuja, L. Dormieux, S. Meille, C. Hellmich, A. Fritsch, Micromechanical explanation of elasticity and strength of gypsum: from elongated anisotropic crystals to isotropic porous polycrystals, J. Eng. Mech. 136 (2010) 239–253, https://doi.org/10.1061/(ASCE)EM.1943-7889.0000072.

[45] J. Gril, D. Jullien, D. Hunt, Compression set and cupping of painted wooden panels. Anal. Characterisation Wooden Cult. Herit. Sci. Eng. Methods, Halle (Saale), Germany, 2016. https://hal.archives-ouvertes.fr/hal-01452161. accessed December 13, 2022.

[46] E. Bosco, A.S.J. Suiker, N.A. Fleck, Crack channelling mechanisms in brittle coating systems under moisture or temperature gradients, Int. J. Fract. 225 (2020) 1–30, https://doi.org/10.1007/s10704-020-00461-3.

[47] A. Kupczak, M. Jędrychowski, M. Strojecki, L. Krzemień, Ł. Bratasz, M.
Łukomski, R. Kozłowski, HERIe: a web-based decision-supporting tool for assessing risk of physical damage using various failure criteria, Stud. Conserv. 63 (2018) 151–155, https://doi.org/10.1080/00393630.2018.1504447.

[48] D. Hunt, Present knowledge of mechano-sorptive creep of wood, creep in Timber Constructions (a state of the art report), Rilem Tech. Comm. 112 (1992) 75–104.

[49] P. Navi, S. Stanzl-Tschegg, Micromechanics of creep and relaxation of wood. A review COST Action E35 2004–2008: wood machining – micromechanics and fracture, HFSG 63 (2009) 186–195, https://doi.org/